Development and metrological evaluation of a microstrip resonator for gas sensing applications

G. Gugliandolo[1], D. Aloisio[2], G. Campobello[3], G. Crupi[4], N. Donato[3]

[1] INRIM, Strada delle Cacce, Torino, Italy, g.gugliandolo@inrim.it
[2] CNR ITAE, Messina, Italy, davide.aloisio@itae.cnr.it
[3] Dept. of Engineering, University of Messina, Italy, gcampobello@unime.it, ndonato@unime.it
[4] Dept. of BIOMORF, University of Messina, Italy, crupig@unime.it

Abstract – **This paper is about the design and the realization of a one-port microwave microstrip resonator working in the frequency range from 3 GHz to 6 GHz and its metrological evaluation in order to be employed as a gas sensor. The prototype can be tailored towards a gas target by depositing an appropriate sensing layer of a nanostructured material. The sensor device is achieved by depositing the sensing material as film layer just on the gap of the resonator. Here, the analysis is focused on an Ag@α-Fe$_2$O$_3$ nanocomposite-based microstrip resonator used for sensing the relative humidity that is varied in the range from 0% to 75%. The increase of humidity value brings to a frequency shift in the two resonances observed in the measured reflection coefficient. The characteristics of the fabricated device suggest its promising use as humidity sensor.**

I. INTRODUCTION

Nowadays, growing attention is being paid to the development of sensors with extremely low-power consumption, in order to meet the increasingly stringent energy-saving requirements of the tremendously expanding market. This can be seen in the recent proliferation of the battery-powered applications, like the wireless sensor networks (WSNs) widely used in environmental (e.g., weather forecasting) [1], industrial (e.g., harmful gases detection) [2], and healthcare (wearable and implantable medical devices) monitoring systems [3,4].

New sensor topologies are continuously proposed to obtain the best achievable trade-off between maximizing performance and functionalities and minimizing power consumption, thereby enabling improvement of the battery lifetime, size, and weight and reduction of the costs. Among the different sensor topologies, microwave sensors are emerging as an attractive solution, owing to their very interesting features, such as fast response time, low-power consumption, full compatibility with wireless communication technologies, and ability to operate at room temperature without the need for a heater.

As well-known, the planar microstrip technology is widely utilized for microwave components (e.g., antennas, resonators, and filters) that find use in various sensing applications, due to its easy fabrication, low cost, and good performance [5-9].

It should be underlined that microwave microstrip sensors are well-suited in particular for gas sensing applications. The operating principle is based on the change in the permittivity of the sensitive material covering the tested structure when the target gas is adsorbed. The recent progress in nanotechnologies have remarkably stimulated the development of gas sensors. Evidence of this can be found in the use of the nanostructured materials as the sensing layers [10-13].

This contribution focuses on the investigation of a one-port microwave microstrip resonator aimed at gas sensing applications. The proposed microstrip resonator consists of three concentric rings with a central disk and is coupled to the microstrip feedline through a small gap. The structure is realized using copper as conductor for the top and ground layers and FR4 as dielectric substrate. An SMA connector is soldered to the input port of the microstrip line for measurement purposes. The reflection coefficient (Γ) of the studied sensor is straightforwardly measured with a conventional vector network analyzer (VNA). The magnitude of Γ exhibits two resonant dips at 3.7 GHz and 5.4 GHz. To assess the resonator performance for gas sensing purposes, humidity monitoring is considered here as a case study. To accomplish this goal, Ag@α-Fe$_2$O$_3$ nanocomposite acting as humidity sensing layer is deposited on the structure under test. The high porosity of the nanostructure enables enhancement of the interaction with water vapour, thus resulting in a higher humidity sensitivity of the developed sensor. As will be shown, variations in humidity can be easily detected and quantified by using the resonant frequency (f_R) values (f_{R1} and f_{R2}) of the two dips appearing in the magnitude of Γ as sensing parameters. As a matter of fact, by gradually increasing the relative humidity (RH) from 0% to 75% at room temperature, both f_{R1} and f_{R2} progressively shift towards lower values. By evaluating the absolute sensitivity (i.e., $S_{fR} = \Delta f_R/\Delta RH$) of the two resonant frequencies of the proposed

sensor, it is found that f_{R2} is the most sensitive parameter for detecting humidity.

II. RESONATOR DESIGN

In this project, a concentric rings microstrip (CRM) resonator was employed as a transducer. This novel resonator topology consists of three concentric copper rings with a 6-mm copper disk in the centre (see Figure 1(d)). A 50-ohm microstrip line was designed as feedline coupled to the resonator through a small gap (of 0.2 mm). This new topology brings some advantages respect to the more classic ring configuration [14,15] since the additional rings increase the resonator quality factor. This enables improvement of the measurement resolution in the detection process.

During the design process, four different geometries have been investigated through computer simulations (see Figure 1): the classic ring resonator (Figure 1 (a)); two concentric copper rings (Figure 1 (b)); three concentric copper rings (Figure 1 (c)); and three concentric copper rings with a central disk (Figure 1 (d)).

(a)

(b)

(c)

(d)
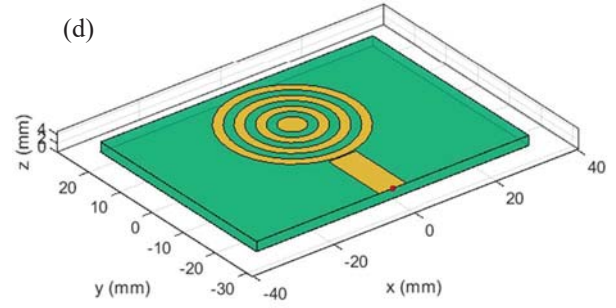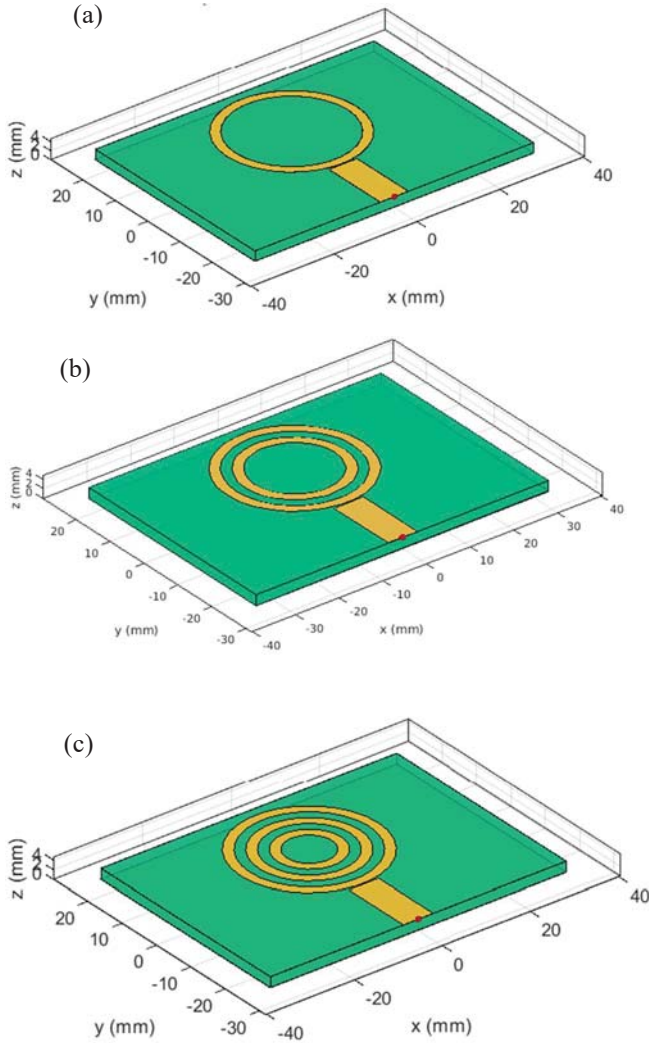
Fig. 1. Illustration of four different resonator topologies.
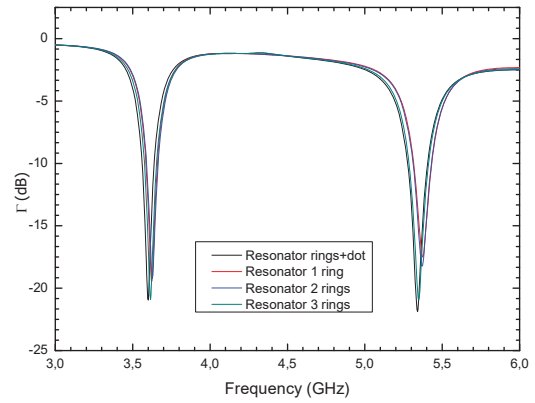
Fig. 2. Simulated reflection coefficient from 3 GHz to 6 GHz for the four resonator topologies.
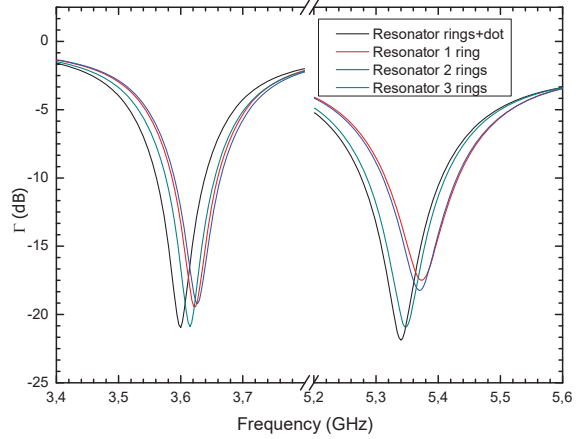
Fig. 3. Illustration of the two dips appearing in the simulated reflection coefficient for the four resonator topologies.

These four resonator topologies exhibited two resonances in the studied frequency range from 3 GHz to 6 GHz. In particular, computer simulations showed a first resonant dip at 3.7 GHz (f_{R1}) and a second dip at 5.4 GHz (f_{R2}). In Figure 2, the magnitude of the simulated Γ is reported for all the four topologies in the frequency range

from 3 GHz to 6 GHz. In Figure 3, the two dips are highlighted by zooming at the frequencies closer to the resonances.

As said before, the main advantage of a CRM resonator respect to the classic ring resonator is that, according to the simulations, the quality factor is higher considering the same resonator size for both geometries.
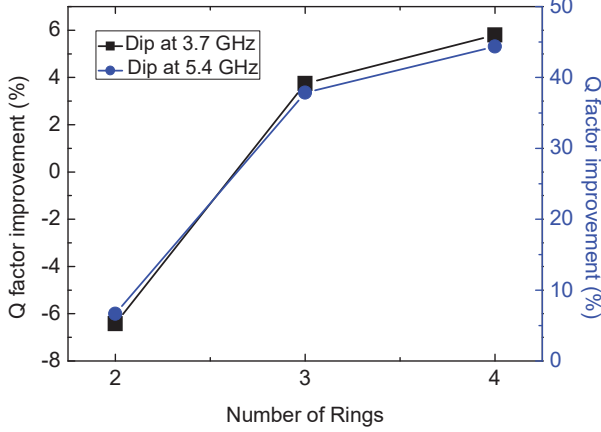
Fig. 4. Variation of the Q factor of two resonances by changing the number of rings of the resonator structure.

As shown in Figure 4, the quality factor, reported as comparison with the singular ring configuration (Figure 1 (a)), increases with the number of concentric rings. In particular, by adding a second ring to the design, the quality factor for the resonant dip at higher frequency is improved by 7%. In the final design (three rings and one disk) the quality factor for the dips at low and high frequency is improved by 6% and 44%, respectively. This last design was selected for fabrication and testing. Measurements on this device are reported in the present paper.

The CRM resonator was fabricated on a 3.2 mm FR4 substrate (ε_r = 4.3, tanδ = 0.025) using copper as conductor for the top and ground layers by means of the Protomat S130 PCB milling machine. An SMA connector was soldered at the end of the feedline as input port and an Agilent 8753ES VNA was used, after calibration, to measure Γ of the device under test.

III. SENSOR PROTOTYPING

After the prototype fabrication and testing, a nanostructured material was deposited on the CRM resonator surface. In particular, an aqueous solution of Ag@α-Fe$_2$O$_3$ nanocomposite was deposited on the gap by drop coating. The description and synthesis of this material is reported in [16].

The sensing material deposition improved the quality factor of both dips by one order of magnitude. A comparison of the Γ before and after the deposition procedure is reported in Figure 5.
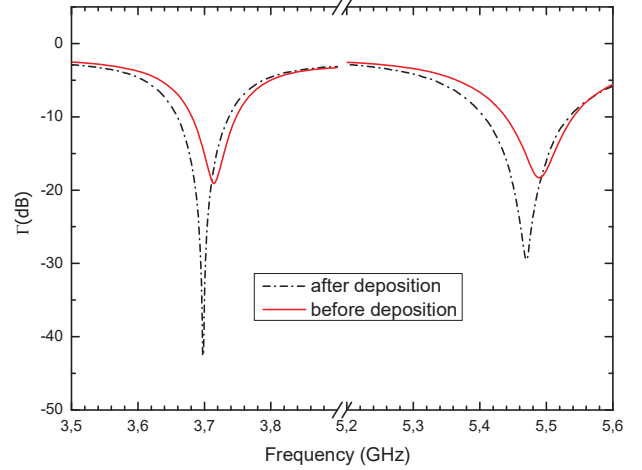
Fig. 5. Measured performance of the studied resonator before and after sensing material deposition.

The resonator was placed inside a plastic chamber and characterized in terms of relative humidity from dry air (0% RH) up to 75% RH. The reflection coefficient was constantly monitored in terms of resonant frequency, Q factor and dip amplitude for the two resonances at each relative humidity set-point. The evaluation of these parameters is described in detail in the next section.

IV. METROLOGICAL EVALUATION

The estimation of the resonant frequency (f_R), Q factor (Q) and dip amplitude (A) from a discrete frequency response is not trivial. A simple linear interpolation of the points constituting the frequency spectrum can provide an inaccurate estimation of these quantities, especially if data are affected by noise. A better approach consists of using a Lorentzian function [17,18] to perform a fitting of the acquired spectrum. From such equation, it is possible to have a good estimation of f_R, Q and A.

In this work the magnitude of the reflection coefficient of the microwave resonator was modelled as a Lorentzian function in the form:

$$|\Gamma(f)| = c_0 - \frac{a_0}{\pi} \cdot \frac{\frac{1}{2}G}{(f-f_R)^2 + \left(\frac{1}{2}G\right)^2} \qquad (1)$$

where: c_0 and a_0 are two real coefficients, G is the full width at half maximum, f_R is the resonant frequency.

From the above equation, A and Q can be calculated respectively as:

$$A = c_0 - a_0 \cdot \frac{2}{\pi G} \qquad (2)$$

$$Q = \frac{f}{\Delta f} = \frac{f_R}{G\sqrt{\sqrt{2}-1}} \qquad (3)$$

where Δf is the resonator half-power bandwidth.

The Levenberg-Marquardt algorithm was employed to fit the Lorentzian function to the measured data points. As shown in Figure 6, the Lorentzian curve fits very well the resonant dip so that it is possible to consider a continuous spectrum and get rid of the noise.

The fitting process allowed an accurate evaluation of the resonator main parameters (f_R, Q, and A) in the whole RH range.
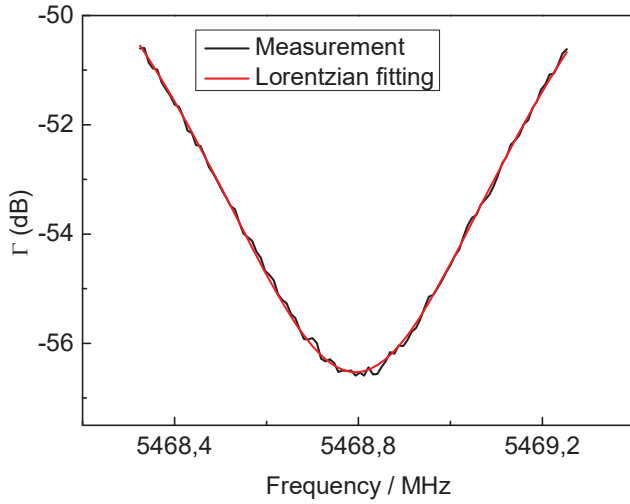
Fig. 6. Resonant dip in the reflection coefficient: measurement (black line) and fitted function (red line).

V. EXPERIMENTAL RESULTS

The microwave device was characterized towards different relative humidity concentrations from 0% RH to 75% RH at room temperature in six steps.

The relative humidity values were set using a fully automated gas control system made by certified gas bottles, permeation tubes and a bubbler inside a thermostatic bath. The three parameters f_R, Q and A have been observed for the whole experimental process.

As regards the Q factor and dip amplitude, no monotonic trends were observed (see Figures 7 and 8). On the other hand, the resonant frequency of both dips seems to be strongly related to the relative humidity concentration (see Figure 9).

A second order polynomial function was used to fit the frequency points with fit residuals within ±100 kHz. Considering an absolute sensitivity S_{fR} of 33 kHz/%RH, this value corresponds to ±3%RH.

The calculated polynomial functions are also reported in Figure 9 for both frequency dips (3.7 GHz value reported on left axis and 5.4 GHz on the right one).
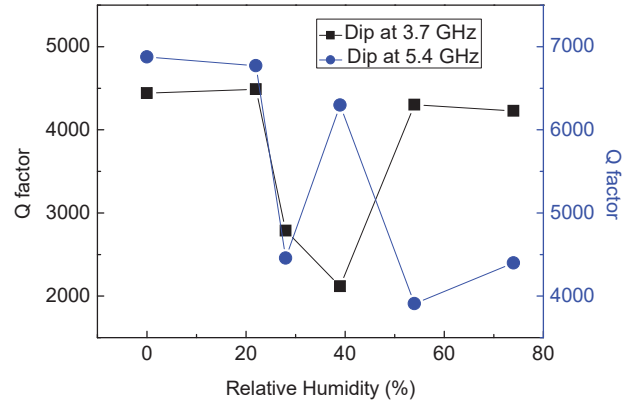
Fig. 7. Quality factor of the two dips in the magnitude of the reflection coefficient at six relative humidity values.
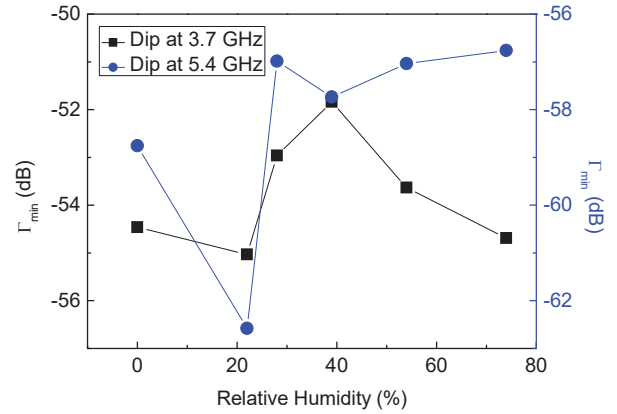
Fig. 8. Amplitudes of the reflection coefficient at the two resonances at six relative humidity values.
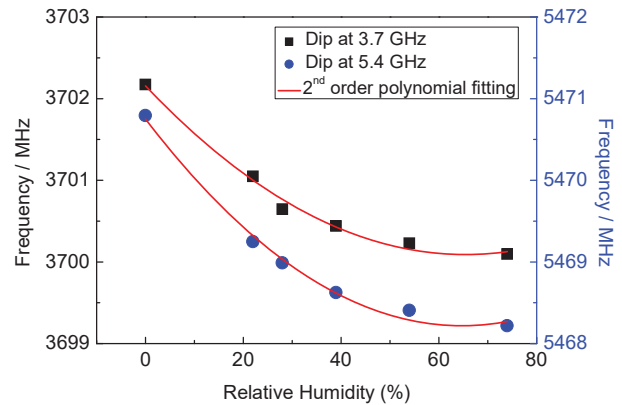
Fig. 9. Resonant frequencies at six relative humidity values with 2nd order polynomial fitting.

VI. CONCLUSIONS

In conclusion, a concentric rings microstrip resonator has been designed, realized, and characterized. The reported simulation data show how the increasing of the number of rings brings to an increasing of the quality factor of the resonator. The microwave transducer was

then tested as sensing device, by depositing a sensing layer of Ag@α-Fe$_2$O$_3$ nano-composite and by recording Γ towards humidity in the range spanning from 0% RH to 75% RH at room temperature. This prototype is a good starting point in order to develop low power gas sensors devices tailored with specific sensing layers.

REFERENCES

[1] G. Campobello, A. Segreto, S. Zanafi and S. Serrano, "RAKE: A simple and efficient lossless compression algorithm for the Internet of Things," 2017 25th European Signal Processing Conference (EUSIPCO), Kos, 2017, pp. 2581-2585, doi: 10.23919/EUSIPCO.2017.8081677.

[2] G. Campobello, M. Castano, A. Fucile, A. Segreto, "WEVA: A complete solution for industrial internet of things," Lect. Notes in Computer Science, Vol. 10517 LNCS, 2017, pp. 231-238.

[3] G. Campobello, A. Segreto, S. Zanafi and S. Serrano, "An Efficient Lossless Compression Algorithm for Electrocardiogram Signals," 2018 26th European Signal Processing Conference (EUSIPCO), Rome, 2018, pp. 777-781, doi: 10.23919/EUSIPCO.2018.8553597.

[4] G. Gugliandolo, G. Campobello, P. P. Capra, S. Marino, A. Bramanti, G. Di Lorenzo, N. Donato, "A Movement-Tremors Recorder for Patients of Neurodegenerative Diseases", IEEE Transactions on. Instrumentation and Measurement, vol. 68, no. 5, pp. 1451-1457, 2019.

[5] G. Bailly, A. Harrabi, J. Rossignol, D. Stuerga, P. Pribetich, "Microwave gas sensing with a microstrip interDigital capacitor: Detection of NH3 with TiO2 nanoparticles," Sensors and Actuators, B: Chemical, vol. 236, pp. 554-564, 2016.

[6] A. Rydosz, E. Maciak, K. Wincza, S. Gruszczynski, Microwave-based sensors with phthalocyanine films for acetone, ethanol and methanol detection, Sensors and Actuators B: Chemical, vol. 237, pp. 876-886, 2016.

[7] G. Barochi, J. Rossignol, M. Bouvet, "Development of microwave gas sensors," Sensors and Actuators B, vol. 157, pp. 374-379, 2011.

[8] M. H. Zarifia,T. Thundat, M. Daneshmand, "High resolution microwave microstrip resonator for sensing applications", Sensors and Actuators A: Physical, vol. 233, pp. 224-230, 2015.

[9] D. Aloisio and N. Donato, "Development of Gas Sensors on Microstrip Disk Resonators", Procedia Engineering, 87, pp. 1083-1086, 2014.

[10] S. B. Tooski, "Sense toxins/sewage gases by chemically and biologically functionalized single-walled carbon nanotube sensor based microwave resonator", J. Appl. Phys. 107, 014702, 2010.

[11] G. Gugliandolo, D. Aloisio, S. G. Leonardi, G. Campobello, N. Donato, "Resonant Devices and Gas Sensing: From Low Frequencies to Microwave Range", Proc, of 14th Int. Conf. TELSIKS 2019, Article n. 9002368, pp. 21-28.

[12] J. Park, T. Kang, B. Kim, et al., "Real-time Humidity Sensor Based on Microwave Resonator Coupled with PEDOT:PSS Conducting Polymer Film", Sci Rep, vol. 8, 439, 2018.

[13] A. Bogner, C. Steiner, S. Walter, J. Kita, G. Hagen, & R. Moos, "Planar Microstrip Ring Resonators for Microwave-Based Gas Sensing: Design Aspects and Initial Transducers for Humidity and Ammonia Sensing", Sensors, vol. 17, no. 10, 2422, 2017.

[14] M.T. Jilani, W. P. Wen, L. Y. Cheong, M. A. Zakariya, M. Z. U. Rehman, "Equivalent circuit modeling of the dielectric loaded microwave biosensor, Radioengineering, vol. 23, no. 4, pp. 1038-1047, 2014.

[15] D. L. Eng, B. C. Olbricht, S. Shi, & D. W. Prather, "Dielectric characterization of thin films using microstrip ring resonators," Microwave and Optical Technology Letters, vol. 57, no. 10, pp. 2306-2310, 2015.

[16] A. Mirzaei, K. Janghorban, B. Hashemi, A. Bonavita, M. Bonyani, S. G. Leonardi, G. Neri, "Synthesis, Characterization and Gas Sensing Properties of Ag@α-Fe$_2$O$_3$ Core-Shell Nanocomposites," Nanomaterials, vol. 5, pp. 737-749, 2015.

[17] P. J. Petersan, S. M. Anlage, "Measurement of Resonant Frequency and Quality Factor of Microwave Resonators: Comparison of Methods", J. of Appl. Physics. 84. 10.1063/1.368498, 1998.

[18] M. P. Robinson and J. Clegg, "Improved determination of Q-factor and resonant frequency by a quadratic curve-fitting method," IEEE Trans. on Electrom. Comp., vol. 47, no. 2, pp. 399-402, 2005.